*J. Fluid Mech.* (1995), *vol.* 283, *pp.* 231–248
Copyright © 1995 Cambridge University Press


# Multi-mode models of flow and of solute dispersion in shallow water. Part 1. General derivation

By RONALD SMITH

Department of Mathematical Sciences, Loughborough University of Technology, LE11 3TU, UK

(Received 23 August 1993 and in revised form 28 May 1994)

Instead of considering just the vertically averaged current and the vertically averaged concentration, a multi-mode model is derived in which more of the vertical structure can be computed directly rather than being lumped into a dispersion coefficient. Test cases, of laminar flows, are used to quantify the accuracy of the lowest non-trivial truncation (two modes) in replicating both the flow and the dispersion process.

## 1. Introduction

After vertical mixing has occurred, solutes are carried along with the vertically averaged flow but the horizontal dispersion depends upon the square of the shear (Taylor 1953). Many different physical effects can contribute to the shear and hence to the horizontal dispersion: bottom drag (Elder 1959), flow curvature (Fischer 1969), buoyancy (Prych 1970), Coriolis effect (Smith 1977) and wind (Fischer 1978). Thus, for (time-dependent) shallow water flows an all encompassing horizontal shear dispersion tensor would involve (time-integral) quadratic combinations of all these physical processes. This paper explores an alternative approach in which some vertical structure of the concentration is calculated and the use of dispersion coefficients is avoided.

Heaps (1972) pioneered the use of spectral (or multi-mode) methods to model the vertical structure of tidal currents and surges in shallow waters. Davies (1987) gives an expository review of subsequent developments. The idea is that the classical shallow water equation for the vertical averaged current is simply the lowest-order truncation in a complete spectral (or multi-mode) representation of the current. The inclusion of more, or a better choice of, modes improves the accuracy and the vertical resolution. The momentum equations and boundary conditions can be used to define natural, efficient and rapidly convergent selections for the modes. Here this approach is extended to encompass the concentration. The different equation and boundary condition for the concentration requires a different set of modes.

The long-term purpose of the present work is to facilitate computationally simple (e.g. two modes) yet acceptably accurate calculations of solute dispersion in real shallow water flows. To quantify the accuracy of using just two modes, detailed comparisons are made for exactly solvable flows. To facilitate general applicability, the derivation includes allowance for time-dependent non-uniform water depth, solute discharges with significant discharges of water and momentum, plus all the physical effects mentioned in the first paragraph of this introduction.

## 2. Sigma coordinates

In shallow waters any vertical velocity $w$ arises principally as a result of changes in depth. An efficient way of accommodating such vertical motion is to use a boundary-following coordinate (Phillips 1957):

$$\sigma = \frac{z+h}{H}, \quad \text{with} \quad H = h+\zeta. \tag{2.1a, b}$$

Here $z$ is the vertical coordinate, the bed is at $z = -h(x,y)$, the free surface is at $z = \zeta(x,y,t)$ and $H(x,y,t)$ is the total water depth. The use of the Greek letter $\sigma$ is conventional and the description 'sigma coordinates' is commonly used. To allow some minor generalizations, this section gives an outline derivation of the mass, momentum and concentration equations in sigma coordinates.

In terms of the horizontal velocity components $u(x,y,\sigma,t)$ and $v(x,y,\sigma,t)$, the vertical velocities at the bed and at the free surface are:

$$w = -u\frac{\partial h}{\partial x} - v\frac{\partial h}{\partial y} \quad \text{at} \quad \sigma = 0, \quad w = \frac{\partial \zeta}{\partial t} + u\frac{\partial \zeta}{\partial x} + v\frac{\partial \zeta}{\partial y} \quad \text{at} \quad \sigma = 1. \tag{2.2a, b}$$

Another source of vertical motion would be the presence of a source of water being discharged at the rate $Q(x,y,\sigma',t)$ into the water column at the fractional height $\sigma'$ above the bed. ($Q$ measures the volume of new water into a unit volume in a unit of time). To accommodate these simple features we replace the conventional vertical velocity $w$ by the quantity $W$:

$$W = \frac{1}{H}\left\{w + (1-\sigma)\left(u\frac{\partial h}{\partial x} + v\frac{\partial h}{\partial y} - H\int_0^\sigma Q\,\mathrm{d}\sigma'\right) - \sigma\left(\frac{\partial \zeta}{\partial t} + u\frac{\partial \zeta}{\partial x} + v\frac{\partial \zeta}{\partial y} - H\int_\sigma^1 Q\,\mathrm{d}\sigma'\right)\right\}. \tag{2.3}$$

In the Boussinesq approximation (in which changes of inertial density are very small but changes in weight may be dynamically significant) the mass conservation equation can be written

$$\frac{\partial \zeta}{\partial t} + \frac{\partial}{\partial x}(Hu) + \frac{\partial}{\partial y}(Hv) + H\frac{\partial W}{\partial \sigma} = H\int_0^1 Q\,\mathrm{d}\sigma'. \tag{2.4}$$

Thus, the change of dependent variable (2.3) has the effect of replacing the local water source strength $Q$ by a vertically averaged source strength. The kinematic boundary conditions for no water flow across the bed $\sigma = 0$ and the free surface $\sigma = 1$ are

$$W = 0 \quad \text{on} \quad \sigma = 0, 1. \tag{2.5}$$

An immediate sequel to (2.4), (2.5) is that the time evolution of the free surface elevation $\zeta(x,y,t)$ is governed by the vertically integrated mass conservation equation

$$\frac{\partial \zeta}{\partial t} + \frac{\partial}{\partial x}\left(H\int_0^1 u\,\mathrm{d}\sigma\right) + \frac{\partial}{\partial y}\left(H\int_0^1 v\,\mathrm{d}\sigma\right) = H\int_0^1 Q\,\mathrm{d}\sigma. \tag{2.6}$$

Also, we can solve (2.4) to give $W$ in terms of the horizontal velocity components $u$, $v$:

$$HW = \frac{\partial}{\partial x}\left(H\left[\sigma\int_\sigma^1 u\,\mathrm{d}\sigma' - (1-\sigma)\int_0^\sigma u\,\mathrm{d}\sigma'\right]\right) + \frac{\partial}{\partial y}\left(H\left[\sigma\int_\sigma^1 v\,\mathrm{d}\sigma' - (1-\sigma)\int_0^\sigma v\,\mathrm{d}\sigma'\right]\right). \tag{2.7}$$

This important result (2.7) makes it possible to take full account of the effects of the vertical velocity within a calculation scheme that only involves the horizontal velocities $u, v$. By contrast, the classical shallow water approximation (Lamb 1945, Chap. 8) corresponds to setting $W$ equal to zero.

In the vertical direction the pressure $p(x, y, \sigma, t)$ is modelled as being hydrostatic (i.e. vertical accelerations are small relative to gravity)

$$p = P + gH\int_{\sigma}^{1} \rho \, \mathrm{d}\sigma'. \tag{2.8}$$

Thus, the water pressure $p$ at a level $\sigma$ balances the atmospheric pressure $P(x, y, t)$ and the weight of a column of water with density $\rho(x, y, \sigma, t)$. The corresponding horizontal momentum equations, with allowance for horizontal momentum sources $M_1$, $M_2$ are

$$\frac{\partial}{\partial t}(Hu)+\frac{\partial}{\partial x}(Hu^2)+\frac{\partial}{\partial y}(Hvu)+H\frac{\partial}{\partial \sigma}(Wu)-Hfv = H(M_1-Qu)-H\left\{\frac{1}{\rho}\frac{\partial P}{\partial x}+g\frac{\partial \zeta}{\partial x}\right\}$$
$$-g\frac{H^2}{\rho}\int_{\sigma}^{1}\frac{\partial \rho}{\partial x}\mathrm{d}\sigma'-\frac{gH}{\rho}\frac{\partial H}{\partial x}\int_{\sigma}^{1}(1-\sigma')\frac{\partial \rho}{\partial \sigma'}\mathrm{d}\sigma'+\frac{1}{H}\frac{\partial}{\partial \sigma}\left(\nu\frac{\partial u}{\partial \sigma}\right), \tag{2.9a}$$

$$\frac{\partial}{\partial t}(Hv)+\frac{\partial}{\partial x}(Huv)+\frac{\partial}{\partial y}(Hv^2)+H\frac{\partial}{\partial \sigma}(Wv)+Hfu = H(M_2-Qv)-H\left\{\frac{1}{\rho}\frac{\partial P}{\partial y}+g\frac{\partial \zeta}{\partial y}\right\}$$
$$-g\frac{H^2}{\rho}\int_{\sigma}^{1}\frac{\partial \rho}{\partial y}\mathrm{d}\sigma'-\frac{gH}{\rho}\frac{\partial H}{\partial y}\int_{\sigma}^{1}(1-\sigma')\frac{\partial \rho}{\partial \sigma'}\mathrm{d}\sigma'+\frac{1}{H}\frac{\partial}{\partial \sigma}\left(\nu\frac{\partial v}{\partial \sigma}\right). \tag{2.9b}$$

Here $f$ is the Coriolis frequency (associated with the rotation of the Earth) and $\nu$ is the eddy viscosity. Additional horizontal viscosity terms (Blumberg & Mellor 1987, equations 37, 38) have been neglected on the premise that the square of the ratio between the water depth and horizontal lengthscales is very small. At the bed a no-slip boundary condition is used:

$$u = v = 0 \quad \text{on} \quad \sigma = 0. \tag{2.10}$$

At the free surface allowance is made for wind stress with components $\tau_1, \tau_2$:

$$\frac{\rho\nu}{H}\frac{\partial u}{\partial \sigma} = \tau_1, \quad \frac{\rho\nu}{H}\frac{\partial v}{\partial \sigma} = \tau_2 \quad \text{on} \quad \sigma = 1. \tag{2.11a, b}$$

In the Boussinesq approximation the density is only a small perturbation $\Delta\rho$ from a reference water density $\rho_0$. Thus, we can replace any derivatives of $\rho$ by derivatives of $\Delta\rho$ and any un-differentiated occurrence of $\rho$ by the constant $\rho_0$.

Despite the inclusion both of depth topography $h(x, y)$ and of a moving free surface $\zeta(x, y, t)$ the above equations (2.9*a*, *b*) look very similar to the widely studied flat-bed, rigid-lid case. Thus (2.9*a*, *b*) provide a good starting point either for full three-dimensional numerical computations (Phillips 1957; Blumberg & Mellor 1987) or for reductions to systems of two-dimensional equations (Heaps 1972; Davies 1987).

For a solute with concentration $c(x, y, \sigma, t)$ and source strength $q(x, y, \sigma, t)$ the advection-diffusion equation takes the form

$$\frac{\partial}{\partial t}(Hc)+\frac{\partial}{\partial x}(Huc)+\frac{\partial}{\partial y}(Hvc)+H\frac{\partial}{\partial \sigma}(Wc)$$
$$= H(q-Qc)+\frac{1}{H}\frac{\partial}{\partial \sigma}\left(\kappa\frac{\partial c}{\partial \sigma}\right)+\frac{\partial}{\partial x}\left(HK\frac{\partial c}{\partial x}\right)+\frac{\partial}{\partial y}\left(HK\frac{\partial c}{\partial y}\right), \tag{2.12a}$$

with $$\kappa \frac{\partial c}{\partial \sigma} = 0 \quad \text{on} \quad \sigma = 0, 1. \tag{2.12b}$$

Here $\kappa$ is the vertical eddy diffusivity and $K$ the horizontal eddy diffusivity. A turbulence $k-\epsilon$ model for $\nu$, $\kappa$, $K$ would involve additional transport equations (Hutton, Smith & Hickmott 1987) which could likewise be solved by appropriate multi-mode expansions.

## 3. Velocity modes

If we are to be efficient in our use of a representation of the vertical structure of the flow, then as far as possible we should build in the mathematical features of the momentum equations (2.9*a*, *b*) and the boundary conditions (2.10), (2.11). Otherwise, computational effort would be wasted in imposing such features as zero flow at the bed. Following Heaps (1972), we give particular emphasis to the eddy viscosity $\nu$ and its approximately universal variation with fractional height above the bed (i.e. constant for laminar flows and parabolic for turbulent flows). If $\hat{\nu}(\sigma)$ is a dimensionless shape function characterizing the idealized eddy viscosity profile in shallow water flows, then we define the velocity modes $\Phi^{(m)}(\sigma)$ and associated eigenvalues $\mu^{(m)}$:

$$\frac{\mathrm{d}}{\mathrm{d}\sigma}\left(\hat{\nu}\frac{\mathrm{d}\Phi^{(m)}}{\mathrm{d}\sigma}\right) + \mu^{(m)}\Phi^{(m)} = 0, \tag{3.1a}$$

with $$\Phi^{(m)} = 0 \quad \text{on} \quad \sigma = 0, \quad \hat{\nu}\frac{\mathrm{d}\Phi^{(m)}}{\mathrm{d}\sigma} = 0 \quad \text{on} \quad \sigma = 1, \tag{3.1b, c}$$

$$\int_0^1 \Phi^{(m)2}\,\mathrm{d}\sigma = 1, \quad \int_0^1 \Phi^{(m)}\Phi^{(n)}\,\mathrm{d}\sigma = 0 \quad \text{for} \quad m \neq n, \tag{3.1d, e}$$

$$\int_0^1 \hat{\nu}\left(\frac{\mathrm{d}\Phi^{(m)}}{\mathrm{d}\sigma}\right)^2 \mathrm{d}\sigma = \mu^{(m)}, \quad \int_0^1 \hat{\nu}\frac{\mathrm{d}\Phi^{(m)}}{\mathrm{d}\sigma}\frac{\mathrm{d}\Phi^{(n)}}{\mathrm{d}\sigma}\,\mathrm{d}\sigma = 0 \quad \text{for} \quad m \neq n. \tag{3.1f, g}$$

For the velocity components $u$, $v$, $W$ we pose the representations

$$u = \sum_{m=0}^{\infty} u^{(m)}(x, y, t)\,\Phi^{(m)}(\sigma), \quad v = \sum_{m=0}^{\infty} v^{(m)}(x, y, t)\,\Phi^{(m)}(\sigma), \tag{3.2a, b}$$

$$HW = \sum_{m=0}^{\infty} \left\{\frac{\partial}{\partial x}(Hu^{(m)}) + \frac{\partial}{\partial y}(Hv^{(m)})\right\}\omega^{(m)}(\sigma), \tag{3.2c}$$

with $$\omega^{(m)}(\sigma) = \sigma\int_\sigma^1 \Phi^{(m)}\,\mathrm{d}\sigma' - (1-\sigma)\int_0^\sigma \Phi^{(m)}\,\mathrm{d}\sigma'. \tag{3.2d}$$

It is the rate of convergence of these series that determines the usefulness of the multi-mode representation (Davies 1987). The vertically integrated mass conservation equation (2.6) now becomes

$$\frac{\partial \zeta}{\partial t} + \sum_{m=0}^{\infty}\left\{\frac{\partial}{\partial x}(Hu^{(m)}) + \frac{\partial}{\partial y}(Hv^{(m)})\right\}\int_0^1 \Phi^{(m)}\,\mathrm{d}\sigma = H\int_0^1 Q\,\mathrm{d}\sigma. \tag{3.3}$$

To derive evolution equations for the velocity amplitude factors $u^{(m)}$, $v^{(m)}$ we multiply the (Boussinesq approximation) momentum equations (2.9*a*, *b*) by $\Phi^{(m)}$ and integrate with respect to $\sigma$:

$$\frac{\partial}{\partial t}(Hu^{(m)})+\sum_j\sum_k\left\{\frac{\partial}{\partial x}(Hu^{(j)}u^{(k)})+\frac{\partial}{\partial y}(Hv^{(j)}u^{(k)})\right\}\int_0^1\Phi^{(j)}\Phi^{(k)}\Phi^{(m)}\,\mathrm{d}\sigma$$
$$-\sum_j\sum_k\left\{\frac{\partial}{\partial x}(Hu^{(j)})+\frac{\partial}{\partial y}(Hv^{(j)})\right\}u^{(k)}\int_0^1\omega^{(j)}\Phi^{(k)}\frac{\mathrm{d}\Phi^{(m)}}{\mathrm{d}\sigma}\,\mathrm{d}\sigma-Hfv^{(m)}$$
$$=H\int_0^1 M_1\Phi^{(m)}\,\mathrm{d}\sigma-H\sum_j u^{(j)}\int_0^1 Q\Phi^{(j)}\Phi^{(m)}\,\mathrm{d}\sigma-H\left\{\frac{1}{\rho_0}\frac{\partial P}{\partial x}+g\frac{\partial\zeta}{\partial x}\right\}\int_0^1\Phi^{(m)}\,\mathrm{d}\sigma$$
$$-\frac{gH^2}{\rho_0}\int_0^1\Phi^{(m)}\int_\sigma^1\frac{\partial\Delta\rho}{\partial x}\,\mathrm{d}\sigma'\,\mathrm{d}\sigma-\frac{g}{\rho_0}H\frac{\partial H}{\partial x}\int_0^1\Phi^{(m)}\int_0^1(1-\sigma')\frac{\partial\Delta\rho}{\partial\sigma'}\,\mathrm{d}\sigma'\,\mathrm{d}\sigma$$
$$+\Phi^{(m)}(1)\frac{\tau_1}{\rho_0}-\sum_j\frac{u^{(j)}}{H}\int_0^1\nu\frac{\mathrm{d}\Phi^{(j)}}{\mathrm{d}\sigma}\frac{\mathrm{d}\Phi^{(m)}}{\mathrm{d}\sigma}\,\mathrm{d}\sigma, \tag{3.4a}$$

$$\frac{\partial}{\partial t}(Hv^{(m)})+\sum_j\sum_k\left\{\frac{\partial}{\partial x}(Hu^{(j)}v^{(k)})+\frac{\partial}{\partial y}(Hv^{(j)}v^{(k)})\right\}\int_0^1\Phi^{(j)}\Phi^{(k)}\Phi^{(m)}\,\mathrm{d}\sigma$$
$$-\sum_j\sum_k\left\{\frac{\partial}{\partial x}(Hu^{(j)})+\frac{\partial}{\partial y}(Hv^{(j)})\right\}v^{(k)}\int_0^1\omega^{(j)}\Phi^{(k)}\frac{\mathrm{d}\Phi^{(m)}}{\mathrm{d}\sigma}\,\mathrm{d}\sigma+Hfu^{(m)}$$
$$=H\int_0^1 M_2\Phi^{(m)}\,\mathrm{d}\sigma-H\sum_j v^{(j)}\int_0^1 Q\Phi^{(j)}\Phi^{(m)}\,\mathrm{d}\sigma-H\left\{\frac{1}{\rho_0}\frac{\partial P}{\partial y}+g\frac{\partial\zeta}{\partial y}\right\}\int_0^1\Phi^{(m)}\,\mathrm{d}\sigma$$
$$-\frac{gH^2}{\rho_0}\int_0^1\Phi^{(m)}\int_\sigma^1\frac{\partial\Delta\rho}{\partial y}\,\mathrm{d}\sigma'\,\mathrm{d}\sigma-\frac{g}{\rho_0}H\frac{\partial H}{\partial y}\int_0^1\Phi^{(m)}\int_0^1(1-\sigma')\frac{\partial\Delta\rho}{\partial\sigma'}\,\mathrm{d}\sigma'\,\mathrm{d}\sigma$$
$$+\Phi^{(m)}(1)\frac{\tau_2}{\rho_0}-\sum_j\frac{v^{(j)}}{H}\int_0^1\nu\frac{\mathrm{d}\Phi^{(j)}}{\mathrm{d}\sigma}\frac{\mathrm{d}\Phi^{(m)}}{\mathrm{d}\sigma}\,\mathrm{d}\sigma. \tag{3.4b}$$

Coupling between the modes in equations (3.4*a*, *b*) arises from the nonlinear advective terms (horizontal and vertical), the density perturbation and the viscosity. Davies (1987) points out that the coupling would be even more complicated and the convergence much slower if the selection (3.1*a–g*) of the modes did not build in suitable boundary conditions and orthogonality. Conversely, if the vertical shape of the velocity profile were known exactly (Falconer 1976) then convergence could be obtained in a single step.

If the eddy viscosity profile $\nu$ is nearly proportional to the idealized dimensionless eddy viscosity profile $\hat{\nu}$:

$$\nu(x,y,\sigma,t)\sim N(x,y,t)\,\hat{\nu}(\sigma), \tag{3.5a}$$

then the viscosity terms in (3.4*a*, *b*) become approximately diagonal

$$-u^{(m)}\frac{N}{H^2}\mu^{(m)}\quad\text{and}\quad-v^{(m)}\frac{N}{H^2}\mu^{(m)}. \tag{3.5b}$$

For weak nonlinearity, it is the growth of $\mu^{(m)}$ with $m$ that determines the rate of convergence of the velocity series (3.2*a*, *b*).

The greatest disparity between the eigenvalues occurs between $m=0$ and $m=1$. So, good predictions of the bulk flow can be expected with just the $m=0$ velocity mode. For example, the classical shallow water (vertically integrated) approximation can be recovered if we put

$$\Phi^{(0)}=1,\quad\omega^{(0)}=0 \tag{3.6a, b}$$

(Lamb 1945, Chap. 8). To get any representation of the shear flow (and dispersion) perpendicular to the bulk flow, it is essential that we also include the $m=1$ mode.

## 4. Concentration modes

For the solute concentration $c(x, y, \sigma, t)$ the different boundary conditions (2.12*b*) require a different family of modes. If $\hat{\kappa}(\sigma)$ is a dimensionless shape function characterizing the idealized eddy diffusivity profile in shallow water flows, then we define the concentration modes $\Psi^{(m)}(\sigma)$ and associated eigenvalues $\lambda^{(m)}$:

$$\frac{\mathrm{d}}{\mathrm{d}\sigma}\left(\hat{\kappa}\frac{\mathrm{d}\Psi^{(m)}}{\mathrm{d}\sigma}\right)+\lambda^{(m)}\Psi^{(m)}=0, \tag{4.1a}$$

with

$$\hat{\kappa}\frac{\mathrm{d}\Psi^{(m)}}{\mathrm{d}\sigma}=0 \quad \text{on} \quad \sigma=0,1, \tag{4.1b}$$

$$\int_0^1 \Psi^{(m)^2}\,\mathrm{d}\sigma=1, \quad \int_0^1 \Psi^{(m)}\Psi^{(n)}\,\mathrm{d}\sigma=0 \quad \text{for} \quad m\neq n, \tag{4.1c,d}$$

$$\int_0^1 \hat{\kappa}\left(\frac{\mathrm{d}\Psi^{(m)}}{\mathrm{d}\sigma}\right)^2\mathrm{d}\sigma=\lambda^{(m)}, \quad \int_0^1 \hat{\kappa}\frac{\mathrm{d}\Psi^{(m)}}{\mathrm{d}\sigma}\frac{\mathrm{d}\Psi^{(n)}}{\mathrm{d}\sigma}\,\mathrm{d}\sigma=0 \quad \text{for} \quad m\neq n. \tag{4.1e,f}$$

The zero mode $\Psi^{(0)}$ is constant (unity) with zero eigenvalue.

In terms of these modes we represent the concentrations as

$$c=\sum_{m=0}^{\infty} c^{(m)}(x,y,t)\,\Psi^{(m)}(\sigma). \tag{4.2}$$

The $\Psi^{(m)}$ component of (2.12*a*) is an evolution equation for $c^{(m)}$:

$$\begin{aligned}
&\frac{\partial}{\partial t}(Hc^{(m)})+\sum_j\sum_k\left\{\frac{\partial}{\partial x}(Hu^{(j)}c^{(k)})+\frac{\partial}{\partial y}(Hv^{(j)}c^{(k)})\right\}\int_0^1 \Phi^{(j)}\Psi^{(k)}\Psi^{(m)}\,\mathrm{d}\sigma\\
&-\sum_j\sum_k\left\{\frac{\partial}{\partial x}(Hu^{(j)})+\frac{\partial}{\partial y}(Hv^{(j)})\right\}c^{(k)}\int_0^1 \omega^{(j)}\Psi^{(k)}\frac{\mathrm{d}\Psi^{(m)}}{\mathrm{d}\sigma}\,\mathrm{d}\sigma\\
&=H\int_0^1 q\Psi^{(m)}\,\mathrm{d}\sigma-H\sum_j c^{(j)}\int_0^1 Q\Psi^{(j)}\Psi^{(m)}\,\mathrm{d}\sigma-\sum_j\frac{c^{(j)}}{H}\int_0^1 \kappa\frac{\mathrm{d}\Psi^{(j)}}{\mathrm{d}\sigma}\frac{\mathrm{d}\Psi^{(m)}}{\mathrm{d}\sigma}\,\mathrm{d}\sigma\\
&+\sum_j\left\{\frac{\partial}{\partial x}\left(H\int_0^1 K\Psi^{(j)}\Psi^{(m)}\,\mathrm{d}\sigma\frac{\partial c^{(j)}}{\partial x}\right)+\frac{\partial}{\partial y}\left(H\int_0^1 K\Psi^{(j)}\Psi^{(m)}\,\mathrm{d}\sigma\frac{\partial c^{(j)}}{\partial y}\right)\right\}.
\end{aligned} \tag{4.3}$$

If the eddy diffusivity is nearly proportional to $\hat{\kappa}$:

$$\kappa\sim N\hat{\kappa}, \tag{4.4}$$

then the $\kappa$-terms in (4.3) become approximately diagonal

$$\frac{-c^{(m)}}{H}\lambda^{(m)}N. \tag{4.5}$$

There is a close similarity between the multi-mode equations (4.3) and the equations for dispersion in a flow with several well-mixed layers (Chickwendu 1986). A truncation involving just the zero mode $c^{(0)}$ has only a single speed and totally neglects the shear dispersion. Hence it is essential to include the $m=1$ mode. The remainder of this paper uses exact results for laminar flows to test the effectiveness of using only the two modes $m=0$ and $m=1$. For simplicity the density perturbation $\Delta\rho$ will be modelled as being proportional to the solute concentration

$$\Delta\rho=\alpha c\rho_0 \tag{4.6}$$

## 5. Trigonometric modes

For constant values of the reference eddy diffusivity and eddy viscosity profiles,

$$\hat{\kappa} = \hat{\nu} = 1, \tag{5.1}$$

the concentration and velocity modes are trigonometric:

$$\Psi^{(0)} = 1, \quad \Psi^{(m)} = \sqrt{2}\cos m\pi\sigma, \quad \lambda^{(m)} = m^2\pi^2, \tag{5.2a–c}$$

$$\Phi^{(m)} = \sqrt{2}\sin((m+\tfrac{1}{2})\pi\sigma), \quad \mu^{(m)} = (m+\tfrac{1}{2})^2\pi^2, \tag{5.3a, b}$$

$$\omega^{(m)} = \frac{\sqrt{2}}{(m+\frac{1}{2})\pi}\{\sigma - 1 + \cos((m+\tfrac{1}{2})\pi\sigma)\}. \tag{5.3c}$$

For the vertically integrated mass conservation equation (3.3) we require the coefficients

$$\int_0^1 \Phi^{(m)}\,\mathrm{d}\sigma = \frac{2\sqrt{2}}{\pi(2m+1)}. \tag{5.4}$$

In a truncation involving just the $m = 0$ and $m = 1$ velocity mode we have

$$\frac{\partial\zeta}{\partial t} + 0.9003\left\{\frac{\partial}{\partial x}(Hu^{(0)}) + \frac{\partial}{\partial y}(Hv^{(0)})\right\} + 0.3001\left\{\frac{\partial}{\partial x}(Hu^{(1)}) + \frac{\partial}{\partial y}(Hv^{(1)})\right\} = H\int_0^1 Q\,\mathrm{d}\sigma, \tag{5.5a}$$

where

$$H = h + \zeta. \tag{5.5b}$$

Thus, most of the horizontal mass flux is associated with the monotonic $m = 0$ velocity mode. (In subsequent equations the coefficients have more complex expressions so a decimal form has been used to make explicit the size and sign of the coefficients.)

For the horizontal momentum equations (3.4*a*, *b*) we require the coefficients

$$\Phi^{(m)}(1) = (-1)^m\sqrt{2}, \tag{5.6a}$$

$$\int_0^1 \Phi^{(j)}\Phi^{(k)}\Phi^{(m)}\,\mathrm{d}\sigma = \frac{1}{\pi\sqrt{2}}\left[\frac{1}{-j+k+m+\frac{1}{2}} + \frac{1}{j-k+m+\frac{1}{2}} + \frac{1}{j+k-m+\frac{1}{2}} - \frac{1}{j+k+m+\frac{3}{2}}\right], \tag{5.6b}$$

$$\int_0^1 \omega^{(j)}\Phi^{(k)}\frac{\mathrm{d}\Phi^{(m)}}{\mathrm{d}\sigma}\,\mathrm{d}\sigma = \frac{2m+1}{(2j+1)\pi\sqrt{2}}\left[\frac{1}{j+k+m+\frac{3}{2}} + \frac{1}{j+k-m+\frac{1}{2}} + \frac{1}{-j+k+m+\frac{1}{2}} - \frac{1}{j-k+m+\frac{1}{2}} - \frac{2(k \neq m)}{k-m} - \frac{2}{m+k+1}\right], \tag{5.6c}$$

$$\int_0^1 \Phi^{(m)}\int_\sigma^1 \Psi^{(j)}\,\mathrm{d}\sigma'\,\mathrm{d}\sigma = \frac{\sqrt{2}}{(m+\frac{1}{2})\pi} + \frac{\sqrt{2}(-1)^{(m+1)}}{(m+\frac{1}{2})^2\pi^2} \quad \text{for } j = 0, \tag{5.6d}$$

$$= \frac{2(-1)^{m+j+1}}{[(m+\frac{1}{2})^2 - j^2]\pi^2} \quad \text{for } j \neq 0, \tag{5.6e}$$

$$\int_0^1 \Phi^{(m)}\int_\sigma^1 (1-\sigma')\frac{\partial\Psi^{(j)}}{\partial\sigma'}\,\mathrm{d}\sigma'\,\mathrm{d}\sigma = 0 \quad \text{for } j = 0, \tag{5.6f}$$

$$= \frac{2(m+\frac{1}{2})}{\pi[(m+\frac{1}{2})^2 - j^2]} + \frac{(-1)^{m+j}4j^2}{[(m+\frac{1}{2})^2 - j^2]^2\pi^2} \quad \text{for } j \neq 0. \tag{5.6g}$$

In (5.6$c$) the term involving ($k \neq m$) is zero when $k = m$. In a truncation involving just two velocity modes and two concentration modes we have

$$\frac{\partial}{\partial t}(Hu^{(0)}) + 1.2004\left\{\frac{\partial}{\partial x}(Hu^{(0)^2}) + \frac{\partial}{\partial y}(Hv^{(0)}u^{(0)})\right\}$$

$$-0.24008\left\{2\frac{\partial}{\partial x}(Hu^{(0)}u^{(1)}) + \frac{\partial}{\partial y}(Hv^{(0)}u^{(1)} + Hv^{(1)}u^{(0)})\right\}$$

$$+0.926\left\{\frac{\partial}{\partial x}(Hu^{(1)^2}) + \frac{\partial}{\partial y}(Hv^{(1)}u^{(1)})\right\} - 0.15005\left\{\frac{\partial}{\partial x}(Hu^{(0)}) + \frac{\partial}{\partial y}(Hv^{(0)})\right\}u^{(0)}$$

$$-0.16505\left\{\frac{\partial}{\partial x}(Hu^{(0)}) + \frac{\partial}{\partial y}(Hv^{(0)})\right\}u^{(1)} + 0.27009\left\{\frac{\partial}{\partial x}(Hu^{(1)}) + \frac{\partial}{\partial y}(Hv^{(1)})\right\}u^{(0)}$$

$$+0.1736\left\{\frac{\partial}{\partial x}(Hu^{(1)}) + \frac{\partial}{\partial y}(Hv^{(1)})\right\}u^{(1)} - Hfv^{(0)}$$

$$= 1.414H\int_0^1 M_1 \sin\left(\frac{\pi\sigma}{2}\right)\mathrm{d}\sigma - Hu^{(0)}\int_0^1 Q(1-\cos\pi\sigma)\,\mathrm{d}\sigma$$

$$-Hu^{(1)}\int_0^1 Q\,(\cos\pi\sigma - \cos 2\pi\sigma)\,\mathrm{d}\sigma - 0.9003H\left\{\frac{1}{\rho_0}\frac{\partial P}{\partial x} + g\frac{\partial\zeta}{\partial x}\right\}$$

$$-0.327\alpha gH^2\frac{\partial c^{(0)}}{\partial x} + 0.2702\alpha gH^2\frac{\partial c^{(1)}}{\partial x} + 1.145\alpha gH\frac{\partial H}{\partial x}c^{(1)} + 1.414\frac{\tau_1}{\rho_0}$$

$$-2.467\frac{u^{(0)}}{H}\int_0^1 \nu(1+\cos\pi\sigma)\,\mathrm{d}\sigma - 7.402\frac{u^{(1)}}{H}\int_0^1 \nu(\cos\pi\sigma + \cos 2\pi\sigma)\,\mathrm{d}\sigma, \quad (5.7a)$$

$$\frac{\partial}{\partial t}(Hv^{(0)}) + 1.2004\left\{\frac{\partial}{\partial x}(Hu^{(0)}v^{(0)}) + \frac{\partial}{\partial y}(Hv^{(0)^2})\right\}$$

$$-0.24008\left\{\frac{\partial}{\partial x}(Hu^{(0)}v^{(1)} + Hu^{(1)}v^{(0)}) + 2\frac{\partial}{\partial y}(Hv^{(0)}v^{(1)})\right\}$$

$$+0.926\left\{\frac{\partial}{\partial x}(Hu^{(1)}v^{(1)}) + \frac{\partial}{\partial y}(Hv^{(1)^2})\right\} - 0.15005\left\{\frac{\partial}{\partial x}(Hu^{(0)}) + \frac{\partial}{\partial y}(Hv^{(0)})\right\}v^{(0)}$$

$$-0.16505\left\{\frac{\partial}{\partial x}(Hu^{(0)}) + \frac{\partial}{\partial y}(Hv^{(0)})\right\}v^{(1)} + 0.27009\left\{\frac{\partial}{\partial x}(Hu^{(1)}) + \frac{\partial}{\partial y}(Hv^{(1)})\right\}v^{(0)}$$

$$+0.1736\left\{\frac{\partial}{\partial x}(Hu^{(1)}) + \frac{\partial}{\partial y}(Hv^{(1)})\right\}v^{(1)} + Hfu^{(0)}$$

$$= 1.414H\int_0^1 M_2 \sin\left(\frac{\pi\sigma}{2}\right)\mathrm{d}\sigma - Hv^{(0)}\int_0^1 Q(1-\cos\pi\sigma)\,\mathrm{d}\sigma$$

$$-Hv^{(1)}\int_0^1 Q(\cos\pi\sigma - \cos 2\pi\sigma)\,\mathrm{d}\sigma - 0.9003H\left\{\frac{1}{\rho_0}\frac{\partial P}{\partial y} + g\frac{\partial\zeta}{\partial y}\right\}$$

$$-0.327\alpha gH^2\frac{\partial c^{(0)}}{\partial y} + 0.2702\alpha gH^2\frac{\partial c^{(1)}}{\partial x} + 1.145\alpha gH\frac{\partial H}{\partial y}c^{(1)} + 1.414\frac{\tau_2}{\rho_0}$$

$$-2.467\frac{v^{(0)}}{H}\int_0^1 \nu(1+\cos\pi\sigma)\,\mathrm{d}\sigma - 7.402\frac{v^{(1)}}{H}\int_0^1 \nu(\cos\pi\sigma + \cos 2\pi\sigma)\,\mathrm{d}\sigma, \quad (5.7b)$$

$$\frac{\partial}{\partial t}(Hu^{(1)})-0.24008\left\{\frac{\partial}{\partial x}(Hu^{(0)^2})+\frac{\partial}{\partial y}(Hv^{(0)}u^{(0)})\right\}$$

$$+0.926\left\{2\frac{\partial}{\partial x}(Hu^{(0)}u^{(1)})+\frac{\partial}{\partial y}(Hv^{(0)}u^{(1)}+Hv^{(1)}u^{(0)})\right\}$$

$$+0.4001\left\{\frac{\partial}{\partial x}(Hu^{(1)^2})+\frac{\partial}{\partial y}(Hv^{(1)}u^{(1)})\right\}+0.405\left\{\frac{\partial}{\partial x}(Hu^{(0)})+\frac{\partial}{\partial y}(Hv^{(0)})\right\}u^{(0)}$$

$$-0.0128\left\{\frac{\partial}{\partial x}(Hu^{(0)})+\frac{\partial}{\partial y}(Hv^{(0)})\right\}u^{(1)}-1.125\left\{\frac{\partial}{\partial x}(Hu^{(1)})+\frac{\partial}{\partial y}(Hv^{(1)})\right\}u^{(0)}$$

$$-0.05\left\{\frac{\partial}{\partial x}(Hu^{(1)})+\frac{\partial}{\partial y}(Hv^{(1)})\right\}u^{(1)}-Hfv^{(1)}$$

$$=1.414H\int_0^1 M_1\sin\left(\frac{3\pi}{2}\sigma\right)\mathrm{d}\sigma-Hu^{(0)}\int_0^1 Q(\cos\pi\sigma-\cos 2\pi\sigma)\,\mathrm{d}\sigma$$

$$-Hu^{(1)}\int_0^1 Q(1-\cos 3\pi\sigma)\,\mathrm{d}\sigma-0.3001H\left\{\frac{1}{\rho_0}\frac{\partial P}{\partial x}+g\frac{\partial\zeta}{\partial x}\right\}$$

$$-0.2364\alpha gH^2\frac{\partial c^{(0)}}{\partial x}+0.1621\alpha gH^2\frac{\partial c^{(1)}}{\partial x}-1.023\alpha gH\frac{\partial H}{\partial x}c^{(1)}-1.414\frac{\tau_1}{\rho_0}$$

$$-7.402\frac{u^{(0)}}{H}\int_0^1\nu(\cos\pi\sigma+\cos 2\pi\sigma)\,\mathrm{d}\sigma-22.2\frac{u^{(1)}}{H}\int_0^1\nu(1+\cos 3\pi\sigma)\,\mathrm{d}\sigma,\quad(5.7c)$$

$$\frac{\partial}{\partial t}(Hv^{(1)})-0.24008\left\{\frac{\partial}{\partial x}(Hu^{(0)}v^{(0)})+\frac{\partial}{\partial y}(Hv^{(0)^2})\right\}$$

$$+0.926\left\{\frac{\partial}{\partial x}(Hu^{(0)}v^{(1)}+Hu^{(1)}v^{(0)})+2\frac{\partial}{\partial y}(Hv^{(0)}v^{(1)})\right\}$$

$$+0.4001\left\{\frac{\partial}{\partial x}(Hu^{(1)}v^{(1)})+\frac{\partial}{\partial y}(Hv^{(1)^2})\right\}+0.405\left\{\frac{\partial}{\partial x}(Hu^{(0)})+\frac{\partial}{\partial y}(Hv^{(0)})\right\}v^{(0)}$$

$$-0.0128\left\{\frac{\partial}{\partial x}(Hu^{(0)})+\frac{\partial}{\partial y}(Hv^{(0)})\right\}v^{(1)}-1.125\left\{\frac{\partial}{\partial x}(Hu^{(1)})+\frac{\partial}{\partial y}(Hv^{(1)})\right\}v^{(0)}$$

$$-0.05\left\{\frac{\partial}{\partial x}(Hu^{(1)})+\frac{\partial}{\partial y}(Hv^{(1)})\right\}v^{(1)}+Hfu^{(1)}$$

$$=1.414H\int_0^1 M_2\sin\left(\frac{3\pi}{2}\sigma\right)\mathrm{d}\sigma-Hv^{(0)}\int_0^1 Q(\cos\pi\sigma-\cos 2\pi\sigma)\,\mathrm{d}\sigma$$

$$-Hv^{(1)}\int_0^1 Q(1-\cos 3\pi\sigma)\,\mathrm{d}\sigma-0.3001H\left\{\frac{1}{\rho_0}\frac{\partial P}{\partial y}+g\frac{\partial\zeta}{\partial y}\right\}$$

$$-0.2364\alpha gH^2\frac{\partial c^{(0)}}{\partial y}+0.1621\alpha gH^2\frac{\partial c^{(1)}}{\partial y}-1.023\alpha gH\frac{\partial H}{\partial y}c^{(1)}-1.414\frac{\tau_2}{\rho_0}$$

$$-7.402\frac{v^{(0)}}{H}\int_0^1\nu(\cos\pi\sigma+\cos 2\pi\sigma)\,\mathrm{d}\sigma-22.2\frac{v^{(1)}}{H}\int_0^1\nu(1+\cos 3\pi\sigma)\,\mathrm{d}\sigma.\quad(5.7d)$$

Much of the superficial complexity of (5.7*a–d*) stems from the allowance for vertical velocities. The many different numerical coefficients are merely consequences of the different vertical profiles of the corresponding terms in the original three-dimensional momentum equations (2.9*a*, *b*). It is only those terms which have exactly the velocity mode structure $\Phi^{(m)}$ that have the coefficient unity. For example, the atmospheric horizontal pressure gradient $(\partial P/\partial x, \partial P/\partial y)$ is independent of $\sigma$, so does not have the requisite $\Phi^{(m)}$ structure and has non-integer coefficients. The viscosity integrals become trivial if $\nu$ conforms with the reference profile (5.1) and does not vary with fractional height $\sigma$ above the bed. Otherwise, the viscosity integrands tend to be weighted towards the bed where viscous terms are more important. It is the rapid increase with $m$ of the viscous coefficients that makes the velocity amplitudes $u^{(0)}, u^{(1)}, \ldots$, decrease sufficiently rapidly for a truncated model to be useful.

For the horizontal concentration advection-mixing equations we require the further coefficients

$$\int_0^1 \Phi^{(j)}\Psi^{(k)}\Psi^{(m)}\,\mathrm{d}s = \frac{2\sqrt{2}}{\pi(2j+1)} \quad \text{for} \quad k=m=0 \tag{5.8a}$$

$$= \frac{2j+1}{\pi[(j+\tfrac{1}{2})^2-m^2]} \quad \text{for} \quad k=0, m\neq 0 \tag{5.8b}$$

$$= \frac{2j+1}{\pi[(j+\tfrac{1}{2})^2-k^2]} \quad \text{for} \quad m=0, k\neq 0 \tag{5.8c}$$

$$= \frac{1}{\pi\sqrt{2}}\left[\frac{1}{j+k+m+\frac{1}{2}} - \frac{1}{k+m-j-\frac{1}{2}} + \frac{1}{j+\frac{1}{2}+k-m} + \frac{1}{j+\frac{1}{2}-k+m}\right] \quad \text{for} \quad k\neq 0, m\neq 0, \tag{5.8d}$$

$$\int_0^1 \omega^{(j)}\Psi^{(k)}\frac{\mathrm{d}\Psi^{(m)}}{\mathrm{d}\sigma}\,\mathrm{d}\sigma = 0 \quad \text{for} \quad m=0, \tag{5.8e}$$

$$= \frac{1}{\pi(j+\frac{1}{2})}\left[2 - \frac{m}{j+\frac{1}{2}-m} - \frac{m}{j+\frac{1}{2}+m}\right] \quad \text{for} \quad k=0, m\neq 0 \tag{5.8f}$$

$$= \frac{m}{(j+\frac{1}{2})\pi\sqrt{2}}\left[\frac{2}{k+m} - \frac{2(k\neq m)}{k-m} - \frac{1}{j+\frac{1}{2}+k+m} + \frac{1}{j+\frac{1}{2}+k-m} - \frac{1}{j+\frac{1}{2}-k+m} + \frac{1}{j+\frac{1}{2}-k-m}\right] \quad \text{for} \quad k\neq 0, m\neq 0. \tag{5.8g}$$

In (5.8*g*) the term involving $(k \neq m)$ is absent when $k = m$. The truncated equations involving just two velocity modes and two concentration modes are

$$\frac{\partial}{\partial t}(Hc^{(0)}) + 0.9003\left\{\frac{\partial}{\partial x}(Hu^{(0)}c^{(0)}) + \frac{\partial}{\partial y}(Hv^{(0)}c^{(0)})\right\} - 0.4244\left\{\frac{\partial}{\partial x}(Hu^{(0)}c^{(1)}) + \frac{\partial}{\partial y}(Hv^{(0)}c^{(1)})\right\}$$

$$+ 0.3001\left\{\frac{\partial}{\partial x}(Hu^{(1)}c^{(0)}) + \frac{\partial}{\partial y}(Hv^{(1)}c^{(0)})\right\} + 0.7639\left\{\frac{\partial}{\partial x}(Hu^{(1)}c^{(1)}) + \frac{\partial}{\partial y}(Hv^{(1)}c^{(1)})\right\}$$

$$= H\int_0^1 (q - Qc^{(0)})\,\mathrm{d}\sigma - 1.414Hc^{(1)}\int_0^1 Q\cos\pi\sigma\,\mathrm{d}\sigma$$
$$+\frac{\partial}{\partial x}\left(H\int_0^1 K\,\mathrm{d}\sigma\frac{\partial c^{(0)}}{\partial x}\right)+1.414\frac{\partial}{\partial x}\left(H\int_0^1 K\cos\pi\sigma\,\mathrm{d}\sigma\frac{\partial c^{(1)}}{\partial x}\right)$$
$$+\frac{\partial}{\partial y}\left(H\int_0^1 K\,\mathrm{d}\sigma\frac{\partial c^{(0)}}{\partial y}\right)+1.414\frac{\partial}{\partial y}\left(H\int_0^1 K\cos\pi\sigma\,\mathrm{d}\sigma\frac{\partial c^{(1)}}{\partial y}\right), \tag{5.9a}$$

$$\frac{\partial}{\partial t}(Hc^{(1)})-0.4244\left\{\frac{\partial}{\partial x}(Hu^{(0)}c^{(0)})+\frac{\partial}{\partial y}(Hv^{(0)}c^{(0)})\right\}+0.8403\left\{\frac{\partial}{\partial x}(Hu^{(0)}c^{(1)})+\frac{\partial}{\partial y}(Hv^{(0)}c^{(1)})\right\}$$
$$+0.7639\left\{\frac{\partial}{\partial x}(Hu^{(1)}c^{(0)})+\frac{\partial}{\partial y}(Hv^{(1)}c^{(0)})\right\}-0.0857\left\{\frac{\partial}{\partial x}(Hu^{(1)}c^{(1)})+\frac{\partial}{\partial y}(Hv^{(1)}c^{(1)})\right\}$$
$$-2.122\left\{\frac{\partial}{\partial x}(Hu^{(0)})+\frac{\partial}{\partial y}(Hv^{(0)})\right\}c^{(0)}+0.08488\left\{\frac{\partial}{\partial x}(Hu^{(1)})+\frac{\partial}{\partial y}(Hv^{(1)})\right\}c^{(0)}$$
$$+0.03001\left\{\frac{\partial}{\partial x}(Hu^{(0)})+\frac{\partial}{\partial y}(Hv^{(0)})\right\}c^{(1)}+0.1929\left\{\frac{\partial}{\partial x}(Hu^{(1)})+\frac{\partial}{\partial y}(Hv^{(1)})\right\}c^{(1)}$$
$$= 1.414H\int_0^1 (q - Qc^{(0)})\cos\pi\,\mathrm{d}\sigma - Hc^{(1)}\int_0^1 Q(1+\cos 2\pi\sigma)\,\mathrm{d}\sigma$$
$$-9.869\frac{c^{(1)}}{H}\int_0^1 \kappa(1-\cos 2\pi\sigma)\,\mathrm{d}\sigma+1.414\frac{\partial}{\partial x}\left(H\int_0^1 K\cos\pi\sigma\,\mathrm{d}\sigma\frac{\partial c^{(0)}}{\partial x}\right)$$
$$+\frac{\partial}{\partial x}\left(H\int_0^1 K(1+\cos 2\pi\sigma)\,\mathrm{d}\sigma\frac{\partial c^{(1)}}{\partial x}\right)+1.414\frac{\partial}{\partial y}\left(H\int_0^1 K\cos\pi\sigma\,\mathrm{d}\sigma\frac{\partial c^{(0)}}{\partial y}\right)$$
$$+\frac{\partial}{\partial y}\left(H\int_0^1 K(1+\cos 2\pi\sigma)\,\mathrm{d}\sigma\frac{\partial c^{(1)}}{\partial y}\right). \tag{5.9b}$$

In shallow waters the square of the ratio between the water depth and horizontal lengthscales is very small. Hence, it is justifiable to neglect the $K$-integrals on the right-hand side of (5.9*b*) by comparison with the $\kappa$-integral term. For the momentum equations (2.9*a*, *b*) such horizontal mixing terms were neglect *a priori*. However, in (5.9*a*) the $\kappa$-integral is absent and it is appropriate to retain the $K$-integrals. Indeed, for a short period immediately after discharge, horizontal diffusion dominates shear dispersion (Gill & Sankarasubramanian 1970).

## 6. Plane Poiseuille and linear Couette flow

The complexity of the mass, momentum and concentration equations (5.5), (5.7), (5.9) is evidence that account is taken of numerous physical effects and their interactions (drag, changes in depth, buoyancy, Coriolis effect, wind stress, time dependence, vertical structure). Thus, there is a profusion of tests that we could make for each effect individually and in combinations. Davies (1987) reviews the extensive testing that has been done concerning velocity predictions. Accordingly, the main thrust of the present paper concerns the testing of concentration predictions. However, before we can calculate the dispersion we need to know the flow.

As a first simple test of the two-mode truncation we consider a steady flow down a gentle slope in water of constant total depth and constant viscosity, with negligible

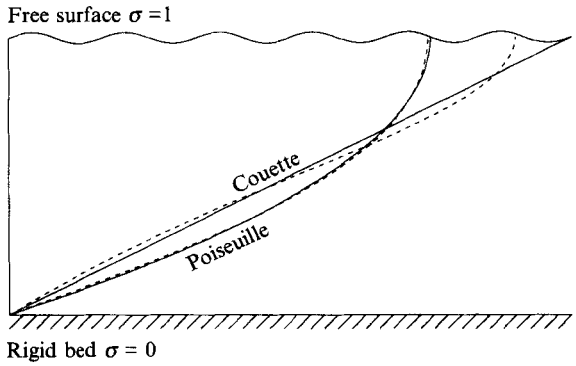


FIGURE 1. Velocity profiles for plane Poiseuille and linear Couette flows (——), with the two-mode approximations (-----).

buoyancy or Coriolis effects. The steady-state solution of the full momentum equations (2.9*a–d*) and boundary conditions (2.10), (2.11) is plane Poiseuille flow

$$u = -\frac{H^2}{\nu} g \frac{\partial \zeta}{\partial x} (\sigma - \tfrac{1}{2}\sigma^2). \tag{6.1}$$

The two-mode momentum equations (5.7*a*, *c*) have the solutions

$$u^{(0)} = -\frac{H^2}{\nu} g \frac{\partial \zeta}{\partial x} \frac{8\sqrt{2}}{\pi^3}, \quad u^{(1)} = -\frac{H^2}{\nu} g \frac{\partial \zeta}{\partial x} \frac{8\sqrt{2}}{27\pi^3}. \tag{6.2a, b}$$

Figure 1 compares the dimensionless velocity profiles (with an extra factor of 3 to bring the average value of the exact profile to 1):

$$3(\sigma - \tfrac{1}{2}\sigma^2) \quad \text{and} \quad \frac{48}{\pi^3}\left[\sin\left(\frac{\pi\sigma}{2}\right) + \frac{1}{27}\sin\left(\frac{3\pi}{2}\sigma\right)\right]. \tag{6.3a, b}$$

The two-mode trigonometric representation for the velocity profile is accurate to within less than 1% of the average velocity.

As a second simple test (of the same two-mode equations) we consider steady wind-driven flow in water of constant depth and constant viscosity, with negligible buoyancy or Coriolis effects. The steady-state exact velocity profile is linear Couette flow

$$u = \frac{\tau_1 H}{\rho_0 \nu} \sigma. \tag{6.4}$$

The corresponding solutions of the two-mode equations are

$$u^{(0)} = \frac{\tau_1 H}{\rho_0 \nu} \frac{4\sqrt{2}}{\pi^2}, \quad u^{(1)} = -\frac{\tau_1 H}{\rho_0 \nu} \frac{4\sqrt{2}}{9\pi^2}. \tag{6.5a, b}$$

Figure 1 compares the dimensionless velocity profiles (with an extra factor of 2):

$$2\sigma \quad \text{and} \quad \frac{16}{\pi^2}\left[\sin\left(\frac{\pi}{2}\sigma\right) - \frac{1}{9}\sin\left(\frac{3\pi}{2}\sigma\right)\right]. \tag{6.6a, b}$$

The accuracy is poor near the free surface.

A discussion of velocity modelling for wind-driven flows is included in the review by Davies (1987). An extreme stance is to use the steady-state wind-driven velocity profile

to determine the modes (Koutitas & Koutita 1986). This guarantees perfect replication of exact results for the idealized cases. The testing should then be for non-idealized cases such as oscillatory flows.

## 7. Tests of the concentration predictions

The majority of exact results for shear dispersion use the method of moments (Aris 1956) in which the single (but daunting) calculation of the concentration distribution is replaced by much simpler (but infinitely many) calculations of the moments: the amount of material, its centroid movement, the amount of spreading, skewness, spikiness, etc. Accordingly, this section compares exact results for the first few moments of the concentration distribution in plane Poiseuille and linear Couette flow with the first few moments of the two-mode model (see the Appendix).

After vertical mixing has taken place, the concentration is carried along at the vertically averaged velocity $\bar{u}$. For plane Poiseuille flow (6.1) and for linear Couette flow (6.4) this velocity is related to the driving forces:

$$\bar{u} = -\frac{H^2}{3\nu} g \frac{\partial \zeta}{\partial x} \quad \text{and} \quad \bar{u} = \frac{\tau_1 H}{2\rho_0 \nu}. \tag{7.1a, b}$$

In the two-mode model the asymptotic velocity of the $c^{(0)}$ mode, when $c^{(1)}$ decays, is (see the Appendix):

$$\frac{2\sqrt{2}}{\pi} u^{(0)} + \frac{2\sqrt{2}}{3\pi} u^{(1)}. \tag{7.2}$$

The results (6.2*a*, *b*) and (6.5*a*, *b*) allow us to relate this velocity to the driving forces

$$-\frac{32}{\pi^4}\left(1+\frac{1}{81}\right)\frac{H^2 g}{\nu}\frac{\partial \zeta}{\partial x} = -0.3325\frac{H^2 g}{\nu}\frac{\partial \zeta}{\partial x}, \tag{7.3a}$$

and

$$\frac{16}{\pi^3}\left(1-\frac{1}{27}\right)\frac{\tau_1 H}{\rho_1 \nu} = 0.4969\frac{\tau_1 H}{\rho_0 \nu}. \tag{7.3b}$$

The differences between these two-mode approximations (7.3*a*, *b*) and the exact results (7.1*a*, *b*) is less than 1%.

Standard shear dispersion models (Taylor 1953) do not account for any centroid displacement associated with the initial vertical discharge profile. For a point release (with negligible volume or momentum but a significant quantity of contaminant) the initial speed of the contaminant matches the flow speed at the release height $\sigma'$. After vertical mixing has taken place there remains a centroid displacement comprising two terms (Aris 1956)

$$G(\sigma') + G(\sigma), \tag{7.4}$$

where $G$ is the centroid displacement function and $\sigma$ is the observation height. For the vertically averaged concentration $\bar{c}$, the observation term $G(\sigma)$ would be absent. For a uniform discharge the release term $G(\sigma')$ is absent. When the vertical diffusivity $\kappa$ is constant, the polynomial velocity profiles (6.1), (6.4) for plane Poiseuille and linear Couette flow lead to polynomial formulae for the corresponding centroid displacement functions $G(\sigma)$:

$$-\frac{H^4 g}{\nu\kappa}\frac{\partial \zeta}{\partial x}\frac{1}{3}\left\{-\frac{1}{15}+\frac{\sigma^2}{2}-\frac{\sigma^3}{2}+\frac{\sigma^4}{8}\right\} \quad \text{and} \quad \frac{\tau_1 H^3}{\rho_0 \nu\kappa}\frac{1}{2}\left\{-\frac{1}{12}+\frac{\sigma^2}{2}-\frac{\sigma^3}{3}\right\}. \tag{7.5a, b}$$

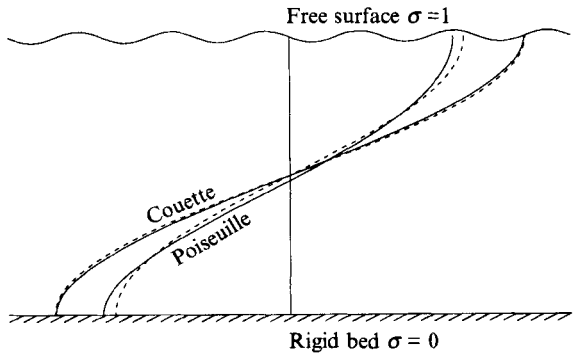


FIGURE 2. Shapes of the centroid displacement functions (——) and the two-mode approximations (-----) for plane Poiseuille and linear Couette flows.

For the two-mode model, equation (A 9) gives the trigonometric formula for the centroid displacement function

$$G(\sigma) = -\frac{H^2}{\pi^2\kappa}\left[\frac{4u^{(0)}}{3\pi} - \frac{12}{5\pi}u^{(1)}\right]\sqrt{2}\cos\pi\sigma. \tag{7.6}$$

The results (6.2*a*, *b*) and (6.5*a*, *b*) allow us to relate this displacement to the driving forces

$$G(\sigma) = \frac{H^4 g}{\nu\kappa}\frac{\partial\zeta}{\partial x}\frac{64}{3\pi^6}[1-\tfrac{1}{15}]\cos\pi\sigma, \tag{7.7a}$$

and

$$G(\sigma) = -\frac{\tau_1 H^3}{\rho_0\nu\kappa}\frac{32}{3\pi^5}[1+\tfrac{1}{5}]\cos\pi\sigma. \tag{7.7b}$$

Figure 2 compares the shapes of exact and approximate centroid displacement functions (7.5), (7.7). It deserves reiteration that standard shear dispersion models neglect centroid displacements.

Bugliarello & Jackson (1964) give the longitudinal shear dispersion coefficient for plane Poiseuille flow

$$D = \frac{2\bar{u}^2H^2}{105\kappa} = 0.0021164\frac{H^6g^2}{\nu^2\kappa}\left(\frac{\partial\zeta}{\partial x}\right)^2. \tag{7.8a}$$

Saffman (1962) gives the longitudinal shear dispersion coefficient for linear Couette flow

$$D = \frac{\bar{u}^2H^2}{30\kappa} = 0.008333\frac{\tau_1^2H^4}{\rho_0^2\nu^2\kappa}. \tag{7.8b}$$

For the two-mode model, equation (A 12) gives the shear dispersion coefficient.

$$D = \left[\frac{4}{3\pi}u^{(0)} - \frac{12}{5\pi}u^{(1)}\right]^2\frac{H^2}{\pi^2\kappa}. \tag{7.9}$$

For the two-mode versions of plane Poiseuille flow (6.2*a*, *b*) and of linear Couette flow (6.5*a*, *b*) the corresponding shear dispersion coefficients are

$$D = 2\left(\frac{32}{3\pi^5}\right)^2\left(1-\frac{1}{15}\right)^2\frac{H^6g^2}{\nu^2\kappa}\left(\frac{\partial\zeta}{\partial x}\right)^2 = 0.0021167\frac{H^6g^2}{\nu^2\kappa}\left(\frac{\partial\zeta}{\partial x}\right)^2, \tag{7.10a}$$

$$D = 2\left(\frac{16}{3\pi^3}\right)^2\left(1+\frac{1}{5}\right)^2\frac{\tau_1^2H^4}{\rho_0^2\nu^2\kappa} = 0.008633\frac{\tau_1^2H^4}{\rho_0^2\nu^2\kappa}. \tag{7.10b}$$

Remarkably, the error in the dispersion coefficients (7.10*a*) for plane Poiseuille flow is only in the fifth significant figure. By contrast, the two-mode dispersion coefficients (7.10*b*) for linear Couette flow are nearly 4% in excess. (This would correspond to a 2% underestimate in the peak concentration at large times.)

Another feature which is omitted in standard shear dispersion models is the initial inefficiency of the shear process (Gill & Sankarasubramanian 1970). The long-term consequence is to give a reduced longitudinal variance. For a uniform discharge at $t = 0$ Chatwin (1970, appendix B) derived the neat result

$$V^{(2)} \sim 2(K+D)\,t - 2\overline{G^2}, \tag{7.11}$$

where $G(\sigma)$ is the centroid displacement function (as given in (7.5*a*, *b*)) and the overbar indicates a cross-sectional (vertical) average value. For plane Poiseuille flow and for linear Couette flow the deficit variance $2\overline{G^2}$ has the values

$$\frac{2}{4725}\left(\frac{H^4 g}{\nu\kappa}\frac{\partial\zeta}{\partial x}\right)^2 = 0.0004233\left(\frac{H^4 g}{\nu\kappa}\frac{\partial\zeta}{\partial x}\right)^2$$

and

$$\frac{17}{10080}\left(\frac{\tau_1 H^3}{\rho_0 \nu\kappa}\right)^2 = 0.001686\left(\frac{\tau_1 H^3}{\rho_0 \nu\kappa}\right)^2. \tag{7.12a, b}$$

The corresponding deficit variance, equation (A13), for the two-mode model is

$$2\left[\frac{4}{3\pi}u^{(0)} - \frac{12}{5\pi}u^{(1)}\right]^2\left(\frac{H^2}{\pi^2\kappa}\right)^2. \tag{7.13}$$

For the two-mode versions of plane Poiseuille flow (6.2*a*, *b*) and of linear Couette flow (6.5*a*, *b*) the respective deficit variances are

$$\left(\frac{64}{3\pi^6}\right)^2\left(1-\frac{1}{15}\right)^2\left(\frac{H^4 g}{\nu\kappa}\frac{\partial\zeta}{\partial x}\right)^2 = 0.0004289\left(\frac{H^4 g}{\nu\kappa}\frac{\partial\zeta}{\partial x}\right)^2, \tag{7.14a}$$

and

$$\left(\frac{32}{3\pi^5}\right)^2\left(1+\frac{1}{5}\right)^2\left(\frac{\tau_1 H^3}{\rho_0 \nu\kappa}\right)^2 = 0.001749\left(\frac{\tau_1 H^3}{\rho_0 \nu\kappa}\right)^2. \tag{7.14b}$$

Again, linear Couette flow has the larger error of nearly 4%.

The method of moments could be pursued further (Chatwin 1970). However, the above tests of the two-mode truncation serve to demonstrate that many features of the exact dispersion process are replicated with reasonable accuracy. In particular, the centroid displacement and deficit variance are features omitted in conventional dispersion models (Taylor 1953).

## 8. Concluding remarks

In a real flow different physical effects can dominate the flow and the dilution process in different places or at different times. Accordingly, the derivation given in this paper of the multi-mode (or two-mode) equations includes a profusion of physical effects and their interactions. Similarly, the testing of the accuracy of the two-mode truncation is for flows with different driving forces.

By calculating some of the vertical structure of the flow and of the concentration, the computational task is more complicated than solving the shallow water equations for the flow and the shear dispersion equation for the concentration. However, features omitted in the shallow water and shear dispersion equations are represented (e.g. cross-flows and the effect of the vertical position of the discharge).

This work would not have been attempted without encouragement and advice from Jerzy Petera and Cecil Scott, who wrote and tested computer codes even before this derivation was finished.

## Appendix. Method of moments

For water with constant vertical diffusivity $\kappa$ the two-mode representation for the concentration is

$$c(x,y,\sigma,t) = c^{(0)}(x,y,t) + c^{(1)}(x,y,t)\sqrt{2}\cos\pi\sigma, \tag{A 1}$$

where $\sigma$ is the fractional height above the bed. If the viscosity is constant, then the two-mode representation for the velocity in the $x$-direction is

$$u = u^{(0)}\sqrt{2}\sin\left(\frac{\pi}{2}\sigma\right) + u^{(1)}\sqrt{2}\sin\left(\frac{3\pi}{2}\sigma\right). \tag{A 2}$$

When the discharge is of negligible volume, momentum or buoyancy, in a unidirectional flow with constant depth $H$ and constant horizontal diffusivity $K$, the two mode equations (5.9$a$, $b$) are

$$\frac{\partial c^{(0)}}{\partial t} + \left[\frac{2\sqrt{2}}{\pi}u^{(0)} + \frac{2\sqrt{2}}{3\pi}u^{(1)}\right]\frac{\partial c^{(0)}}{\partial x} - \left[\frac{4}{3\pi}u^{(0)} - \frac{12}{5\pi}u^{(1)}\right]\frac{\partial c^{(1)}}{\partial x} = q^{(0)} + K\frac{\partial^2 c^{(0)}}{\partial x^2} + K\frac{\partial^2 c^{(0)}}{\partial y^2}, \tag{A 3$a$}$$

$$\frac{\partial c^{(1)}}{\partial t} + \left[\frac{28\sqrt{2}}{15\pi}u^{(0)} - \frac{4\sqrt{2}}{21\pi}u^{(1)}\right]\frac{\partial c^{(1)}}{\partial x} + \frac{\pi^2}{H^2}\kappa c^{(1)} - \left[\frac{4}{3\pi}u^{(0)} - \frac{12}{5\pi}u^{(1)}\right]\frac{\partial c^{(0)}}{\partial x} = q^{(1)}. \tag{A 3$b$}$$

Here the discharge strengths for the two modes are related to the vertical distribution of the discharge strength $q(x,y,\sigma,t)$:

$$q^{(0)} = \int_0^1 q\,\mathrm{d}\sigma, \quad q^{(1)} = \int_0^1 q\sqrt{2}\cos\pi\sigma\,\mathrm{d}\sigma. \tag{A 4$a$, $b$}$$

Following Aris (1956), we define spatial moments relative to the natural velocity of the $c^{(0)}$ mode:

$$c_{m,n}(\sigma,t) = \int_{-\infty}^{\infty}\int_{-\infty}^{\infty}\left(x - \int_0^t\left[\frac{2\sqrt{2}}{\pi}u^{(0)}(t') + \frac{2\sqrt{2}}{3\pi}u^{(1)}(t')\right]\mathrm{d}t'\right)^m y^n c\,\mathrm{d}x\,\mathrm{d}y. \tag{A 5}$$

In terms of the moments, the partial differential equations (A 3$a$, $b$) are replaced by a sequence of ordinary differential equations:

$$\frac{\mathrm{d}c^{(0)}_{m\,n}}{\mathrm{d}t} = -m\left[\frac{4}{3\pi}u^{(0)} - \frac{12}{5\pi}u^{(1)}\right]c^{(1)}_{m-1,\,n} + q^{(0)}_{m,\,n} + m(m-1)\,Kc_{m-2,\,n} + n(n-1)\,Kc_{m,\,n-2}, \tag{A 6$a$}$$

$$\frac{\mathrm{d}c^{(1)}_{m\,n}}{\mathrm{d}t} + \frac{\pi^2\kappa}{H^2}c^{(1)}_{m,\,n} = -m\left[\frac{4}{3\pi}u^{(0)} - \frac{12}{5\pi}u^{(1)}\right]c^{(0)}_{m-1,\,n} - m\left[\frac{2\sqrt{2}}{15\pi}u^{(0)} + \frac{6\sqrt{2}}{7\pi}u^{(1)}\right]c^{(1)}_{m-1,\,n} + q^{(1)}_{m,\,n}. \tag{A 6$b$}$$

For simplicity, we shall restrict our attention to steady flows and to instantaneous discharges at time $t = 0$ and longitudinal position $x = 0$.

The zero moments have the solutions

$$c_{0,0}^{(0)}(t) = q_{0,0}^{(0)}, \quad c_{0,0}^{(1)} = q_{0,0}^{(1)} \exp\left(-\frac{\pi^2}{H^2}\kappa t\right) \quad \text{for} \quad t > 0. \tag{A 7a, b}$$

Thus, the amount of material $Hc_{0,0}^{(0)}$ in the flow remains constant while the vertical non-uniformity decays exponentially on the vertical mixing time and is proportional to the initial non-uniformity $q^{(1)}$ of the discharge.

The first moments with respect to $x$ have the solutions

$$c_{1,0}^{(0)}(t) = -\frac{H^2}{\pi^2\kappa} q_{00}^{(1)} \left[\frac{4}{3\pi}u^{(0)} - \frac{12}{5\pi}u^{(1)}\right]\left[1 - \exp\left(-\frac{\pi^2}{H^2}\kappa t\right)\right], \tag{A 8a}$$

$$c_{1,0}^{(0)}(t) = -\frac{H^2}{\pi^2\kappa} q_{00}^{(0)} \left[\frac{4}{3\pi}u^{(0)} - \frac{12}{5\pi}u^{(1)}\right]\left[1 - \exp\left(-\frac{\pi^2}{H^2}\kappa t\right)\right]$$
$$- q_{0,0}^{(1)} \left[\frac{2\sqrt{2}}{15\pi}u^{(0)} + \frac{6\sqrt{2}}{7\pi}u^{(1)}\right] t \exp\left(-\frac{\pi^2}{H^2}\kappa t\right). \tag{A 8b}$$

Non-zero values of the first moment imply that not all of the centroid movement is accounted for in the natural velocity of the $c^{(0)}$ mode. At large times after discharge the extra centroid displacement (as a function of $\sigma$) is

$$\frac{c_{1,0}}{c_{0,0}} \sim -\frac{H^2}{\pi^2\kappa}\left[\frac{4u^{(0)}}{3\pi} - \frac{12}{5\pi}u^{(1)}\right]\left\{\frac{\sqrt{2}}{q_{0,0}^{(0)}}\int_0^1 q \cos \pi\sigma' \, \mathrm{d}\sigma' + \sqrt{2}\cos \pi\sigma\right\}. \tag{A 9}$$

Aris (1956) pointed out that for a delta-function discharge at fractional height $\sigma'$ there is the same functional form for the centroid displacement with respect to discharge height $\sigma'$ and observational height $\sigma$.

For $c^{(0)}$ the solution for the second moment with respect to $x$ is

$$c_{2,0}^{(0)} = 2\left[\frac{4u^{(0)}}{3\pi} - \frac{12}{5\pi}u^{(1)}\right]^2 \frac{H^2}{\pi^2\kappa}\left\{t - \left[1 - \exp\left(-\frac{\pi^2}{H^2}\kappa t\right)\right]\frac{H^2}{\pi^2\kappa}\right\} q_{0,0}^{(0)}$$
$$+ \frac{2q_{0,0}^{(1)}}{\pi^4\kappa^2} H^4 \left[\frac{4u^{(0)}}{3\pi} - \frac{12}{5\pi}u^{(1)}\right]\left[\frac{2\sqrt{2}}{15\pi}u^{(0)} + \frac{6\sqrt{2}}{7\pi}u^{(1)}\right]\left\{1 - \left[1 + \frac{\pi^2}{H^2}\kappa t\right]\exp\left(-\frac{\pi^2}{H}\kappa t\right)\right\}$$
$$+ 2Kt. \tag{A 10}$$

For a uniform discharge the variance $V^{(0)}$ for the zero mode has the asymptote

$$V^{(0)} = \frac{c_{2,0}^{(0)}}{c_{0,0}^{(0)}} - \left(\frac{c_{1,0}^{(0)}}{c_{0,0}^{(0)}}\right)^2$$
$$\sim 2\left(K + \left[\frac{4u^{(0)}}{3\pi} - \frac{12}{5\pi}u^{(1)}\right]^2 \frac{H^2}{\pi^2\kappa}\right)t - 2\frac{H^4}{\pi^4\kappa^2}\left[\frac{4u^{(0)}}{3\pi} - \frac{12}{5\pi}u^{(1)}\right]^2. \tag{A 11}$$

Thus, the horizontal diffusion $K$ is augmented by a quadratic shear dispersion coefficient

$$D = \left[\frac{4u^{(0)}}{3\pi} - \frac{12}{5\pi}u^{(1)}\right]^2 \frac{H^2}{\pi^2\kappa}. \tag{A 12}$$

Also, there is a quadratic deficit variance

$$2\frac{H^4}{\pi^4\kappa^2}\left[\frac{4u^{(0)}}{3\pi} - \frac{12}{5\pi}u^{(1)}\right]^2 \tag{A 13}$$

related to the initial inefficiency of the shear dispersion process (Gill & Sankarasubramanian 1970; Chatwin 1970).

The method of moments can be continued to higher moments (Chatwin 1970). However, the above results provide us with a reasonable number of tests to compare the exact and two-mode approximations for the natural velocity, centroid displacement, shear dispersion and deficit variance.

## REFERENCES


ARIS, R. 1956 On the dispersion of a solute in a fluid flowing through a tube. *Proc. Roy. Soc. Lond.* A **235**, 67–77.

BLUMBERG, A. F. & MELLOR, G. L. 1987 A description of a three-dimensional coastal ocean circulation model. In *Three-dimensional Coastal Ocean Models* (ed. N. S. Heaps), pp. 1–16. AGU.

BUGLIARELLO, G. & JACKSON, E. D. 1964 Random walk study of convective diffusion. *Engng Mech. Div. ASCE* **90**, 49–77.

CHATWIN, P. C. 1970 The approach to normality of the concentration distribution of a solute in solvent flowing along a pipe. *J. Fluid Mech.* **43**, 321–352.

CHICKWENDU, S. C. 1986 Calculation of longitudinal shear dispersivity using an $N$-zone model as $N \to \infty$. *J. Fluid Mech.* **167**, 19–30.

DAVIES, A. M. 1987 Spectral models in continental shelf sea oceanography. *Three-dimensional Coastal Ocean Models* (ed. N. S. Heaps), pp. 71–106. AGU.

ELDER, J. W. 1959 The dispersion of marked fluid in turbulent shear flow. *J. Fluid Mech.* **5**, 544–560.

FALCONER, R. A. 1976 Mathematical modelling of jet-forced circulation in reservoirs and harbours. Ph.D thesis, Imperial College, London.

FISCHER, H. B. 1969 The effects of bends on dispersion in streams. *Water Resources Res.* **5**, 496–506.

FISCHER, H. B. 1978 On the tensor form of the bulk dispersion coefficient in a bounded skewed shear flow. *J. Geophys. Res.* **83**, 2373–2375.

GILL, W. N. & SANKARASUBRAMANIAN, R. 1970 Exact analysis of unsteady convective diffusion. *Proc. Roy. Soc. Lond.* A **316**, 341–350.

HEAPS, N. S. 1972 On the numerical solution of the three-dimensional hydrodynamical equations for tides and storm surges. *Mem. Soc. Sci. Liege.* (6), **2**, 143–180.

HUTTON, A. G., SMITH, R. M. & HICKMOTT, S. 1987 The computation of turbulent flows of industrial complexity by the finite element method – progress and prospects. *Finite Element Fluids* **7**, 289–309.

KOUTITAS, C. & KOUTITA, M. G. 1986 A comparative study of three mathematical models for wind-generated circulation in coastal areas. *Coastal Engng* **10**, 127–138.

LAMB, H. 1945 *Hydrodynamics*. Cambridge University Press.

PHILLIPS, N. A. 1957 A coordinate system having some special advantages for numerical forecasting. *J. Met.* **14**, 184–186.

PRYCH, E. A. 1970 Effect of density differences on lateral mixing in open-channel flow. *Keck Lab. Hydraul. Water Res. Calif. Inst. Tech. Rep.* KH-R-21.

SAFFMAN, P. G. 1962 The effect of wind shear on horizontal spread from an instantaneous ground source. *Q. J. R. Met. Soc.* **88**, 382–393.

SMITH, R. 1977 Coriolis, curvature and buoyancy effects upon dispersion in a narrow channel. *Hydrodynamics of Estuaries and Fjords* (ed. J. C. J. Nihoul), pp. 217–231. Elsevier.

TAYLOR, G. I. 1953 Dispersion of soluble matter in solvent flowing slowly through a tube. *Proc. Roy. Soc. Lond.* A **219**, 186–203.